Mater. Res. Soc. Symp. Proc. Vol. 1741 © 2015 Materials Research Society
DOI: 10.1557/opl.2015.86

Discrete dislocation dynamics simulations of twin size-effects in magnesium

Haidong Fan[1,2*], Sylvie Aubry[3], A. Arsenlis[3], Jaafar A. El-Awady[1*]
[1] Department of Mechanical Engineering, Johns Hopkins University, Baltimore, MD 21218, USA
[2] Department of Mechanics, Sichuan University, Chengdu, Sichuan 610065, P. R. China
[3] Condensed Matter and Materials Division, Lawrence Livermore National Laboratory, Livermore, CA 94551-0808, USA
[*] E-mails: haidongfan8@foxmail.com (H. Fan), jelawady@jhu.edu (J. A. El-Awady)

ABSTRACT

A dislocation-$\{10\bar{1}2\}$ twin boundary (TB) interaction model was proposed and introduced into discrete dislocation dynamics simulations to study the mechanical behavior of micro-twinned Mg. Strong strain hardening was captured by current simulations, which is associated with the strong TB's barrier effect. In addition, twin size effects with small TB spacing leading to a strong yield stress, were observed to be orientation dependent. Basal slip orientation produces a strong size effect, while prismatic slip does a weak one.

INTRODUCTION

As the lightest structural metal, magnesium (Mg) and its alloys have been of practical interest due to their potential use in automotive, aerospace and defense applications. Magnesium has a hexagonal closed packed (HCP) lattice structure with low crystal symmetry, thus, in addition to dislocation-mediated plasticity, twinning is very common and plays an important role in its plastic deformation [1]. However, a full understanding of the dislocation-twin boundary (TB) strengthening is still lacking. Jiang et al. [2] observed that intersections between primary and secondary $\{10\bar{1}2\}$ twins result in significant grain refinement and strong hardening. In addition, Knezevic et al. [3] showed that compression twins in the tension-twinned grains attribute to the hardening behavior. Moreover, Barnett et al. [4] observed the formation of low angle boundaries arising from the dislocation-TB interaction, which act as a source of strengthening. Recently, Fan et al. [5] showed a competition exists between dislocation-TB induced hardening and twinning deformation induced softening.

Over the past two decades, discrete dislocation dynamics (DDD) has been one of the most efficient methods to capture dislocation-mediated plasticity at the micro scale [6-10]. It has been successfully used to study crystal size effects [11, 12], grain size effects [13, 14] and intermittent behavior [15] of the FCC and BCC materials. More recently, DDD simulations of Mg investigated a number of important effects including: dislocation junction formation and strength [16, 17], orientation influence on the grain size effects [18], micro/nano-pillar plasticity [19], elastic anisotropy [20] and Peierls stress [21]. Nevertheless, in all these studies, twinning deformation was not considered. However, twinning plays an important and sometimes dominant role in the mechanical behavior of both single crystals and polycrystals. As a result, such DDD simulations without twinning may lead to inaccurate predication of the mechanical behavior of HCP materials. This indicates the importance and urgency of introducing dislocation-TB interactions into the DDD framework to study the deformation twinning.

In order to address the TB strengthening in Mg, we have recently proposed a systematic interaction model between dislocations and $\{10\bar{1}2\}$ TBs [5]. The model has been successfully integrated into the 3D-DDD code, ParaDiS [8]. In this work, this model is utilized to study the twin size effects and their orientation influence.

SIMULATIONAL MODEL

A cubical simulation cell having edge length l, with periodic boundary conditions (PBCs) imposed along all three directions is employed, as shown in 2D by the inset in Fig. 1. A twin lamella having thickness l_t is introduced vertically at the center of the simulation cell. In this work, only $\{10\bar{1}2\}$ tension twins are considered, as shown by the orientations of the matrix and the twin in Fig. 1. All current simulations were conducted using the 3D-DDD simulation code, ParaDis [8]. Basic Mg parameters used in the current simulations include: shear modulus, G = 17 GPa; Poission ratio, ν = 0.29; magnitude of <*a*> dislocation Burgers vector, b = 0.325 *nm*; axial ratio, *c/a* = 1.6236; and mass density, ρ = 1738 kg/m^3.

A bi-linear law for the dislocation mobility that is fitted to MD simulations of the dislocation mobility in Mg [22] is employed, as discussed in [5]. In addition, uniaxial strain-controlled loading with a constant strain rate of $\dot{\varepsilon} = -5000/\mathrm{s}$ was imposed in the current simulations. Due to the configuration symmetry along the *x* and *z* axes with respect to the twin lamella, the loading axis is limited to be on the *yz* plane. As a result, two representative loading directions denoted by *z*, and *yz* are considered. Loading along the *z* direction is realized by imposing a strain rate $\dot{\varepsilon}_z = \dot{\varepsilon}$, while the *yz* loading is a uniaxial loading that is 45º from either the *y* or *z* axis.

Initially, Frank-Read (FR) dislocation sources were randomly distributed within the simulation cell. The initial dislocation source density in all simulations was chosen as $\rho_{src} = 5\times10^{12}$ m^{-2}, and the FR source length was l_{src} = 0.26 μm. While dislocation slip on various slip planes is possible in HCP crystals, ⟨*a*⟩ dislocations on basal, prismatic and pyramidal I planes as well as ⟨*c*+*a*⟩ dislocations on pyramidal II planes play a predominant role in dislocation mediated plasticity in Mg [23, 24]. Therefore, in the current simulations all dislocation sources were initially assigned on these specific four slip planes with equal numbers, which also agree with previous studies [18, 25]. The experimentally measured Peierls stresses for dislocations on the basal (0.52 MPa), prismatic (39.2 MPa), and pyramidal planes (105 MPa) were introduced into the code. These values are also in good agreement with recent molecular dynamics (MD) predictions [22 , 26]. To account for possible statistical variations due to the random distribution of dislocation sources, each simulation was repeated three times with different initial distributions.

In [5], we have developed a systematic interaction model between dislocations and $\{10\bar{1}2\}$ tension TBs. In that model, geometric and power dissipation rules are specified in details. All the possible incident dislocations (<*a*>, <*c*> and <*c*+*a*>) from any slip planes (basal, prismatic, pyramidal I and pyramidal II planes) interacting with the $\{10\bar{1}2\}$ tension twin boundary were considered.

RESULTS AND DISCUSSIONS

The stress-strain responses of twinned crystals for the two loading orientations are shown in Fig. 1. Here, the sizes of simulation cells are varied from 0.81 μm to 1.46 μm to study the effects of twin size (TB spacing $l_t = 0.5l$). It can be seen that both orientations show a strong hardening.

For z loading, a strong twin size effect is captured, i.e. smaller is stronger. However, yz loading displays a weak size dependence.

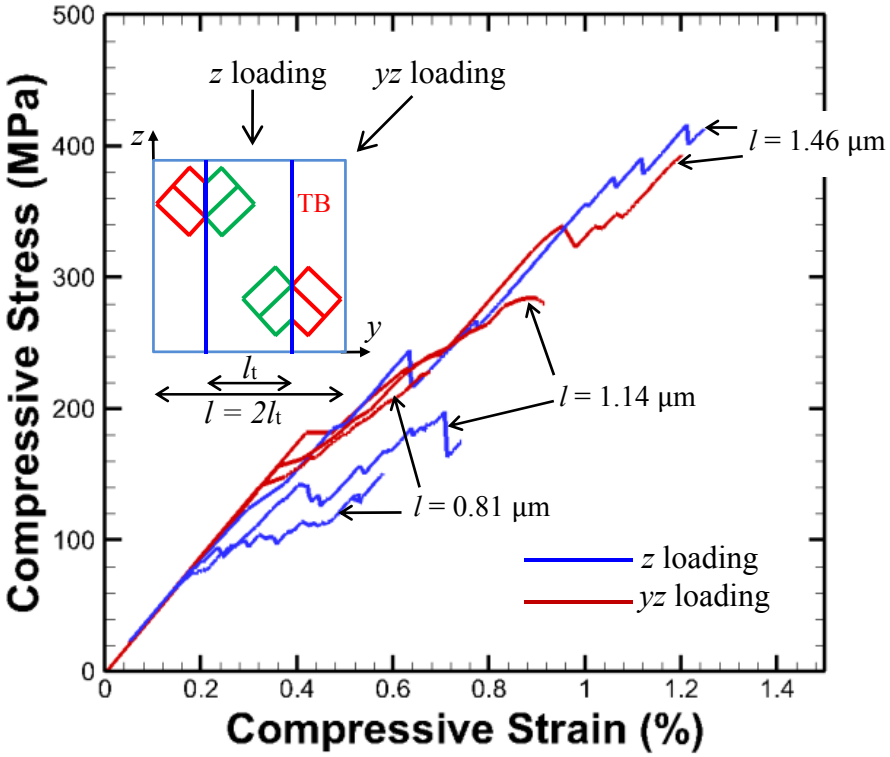

Figure 1. Stress-strain response of twinned crystals with different loading orientations and sizes.

In order to identify the influence of the orientation on the twin size effects, the deformation mechanism of each orientation should be investigated. Figure 2 shows the dislocation configurations for these two orientations. In Fig. 2(a), many parallel dislocations are observed piled-up against the TB during z loading, which indicates that tension TBs are strong barriers to dislocations for this loading. On the contrary, in Fig. 2(b), dislocation pileups are rarely seen. Instead, many intersecting residual dislocations are observed on the TB. The dislocations on TB are seen to belong to one of two types, straight or curve ones.

To compare the size effect intensities of these two orientations, the yield stress is shown in figure 3 as a function of twin size (TB spacing). In addition, a power-law function is used to fit the simulation data. Clearly z loading displays a strong size effect with a power-law exponent of 1.2, while a weak size effect with an exponent 0.4 is observed for yz loading. It should be noted that in [27] an opposite twin size effect (smaller is weaker) was reported for nano-twinned Mg from MD simulations. This can be explained based on that in the current DDD simulations of micro-twinned crystals TBs are strong dislocation obstacles, however, in the nano-twinned Mg TBs act as favorite for dislocation nucleation [27].

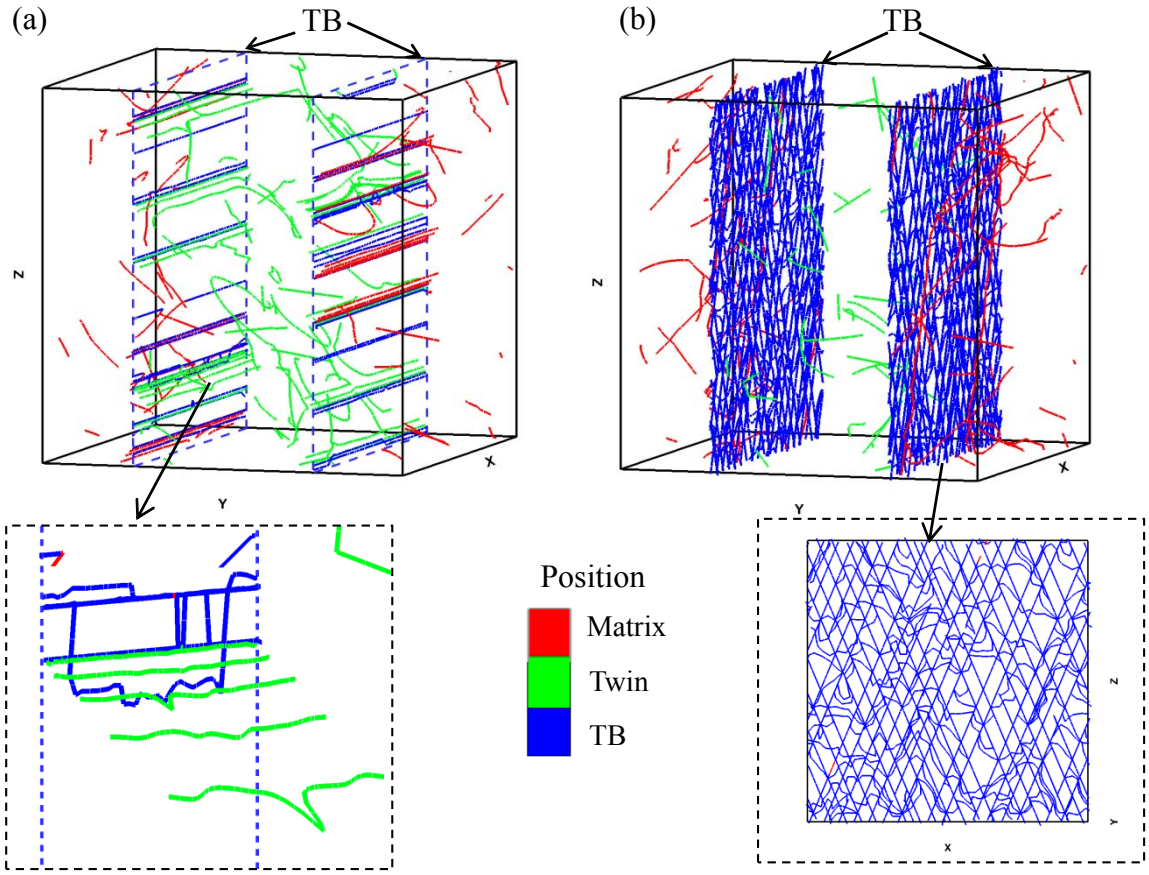

Figure 2. Dislocation configurations in twinned crystals loaded in the (a) z and (b) yz directions.

In Fig. 2(a) during *z* loading, both the basal planes in the matrix and twin make a 46.85° angle with respect to the loading axis, thus plasticity is facilitated mainly by basal slip. Therefore, all the piled up dislocations are basal $\langle a_2 \rangle$ and $\langle a_3 \rangle$ dislocations, since the Schmid factor of $\langle a_1 \rangle$ is 0. When the first dislocation arrives at the TB, it decomposes into one half $\langle c+a \rangle$ dislocation and a twinning dislocation. This decomposition is identical to that reported by MD simulations [28-31] and predicted experimentally [32, 33]. However, the half $\langle c+a \rangle$ dislocation is a sessile dislocation that will remain on the TB. This residual dislocation has a repulsive interaction with subsequent incident dislocations, which contributes to the dislocation pileups near the TB (see inset in Fig. 2). This is one reason for the strong barrier effect of the tension TB. Due to the dislocation pileups at the TB, decreasing the TB spacing leads to strong strengthening through the Hall-Petch effect. That's why a strong twin size effect is observed in Fig. 3.

According to the orientations shown in Fig. 1, during loading along the *yz* direction, the matrix is in a prismatic slip orientation, while the twin is in the harder pyramidal slip orientation. Thus, plasticity is mediated by prismatic $\langle a \rangle$ dislocations in the matrix. Therefore, the straight dislocations on TB in figure 2(b) are half $\langle c+a \rangle$ residual dislocations [5]. Furthermore, the curved dislocations are twinning dislocations, which are glissile on the TB since the Schmid factor is nonzero for this orientation. Few dislocation pileups are observed in Fig. 2(b), indicating a weak twin size effect as shown in Fig. 3.

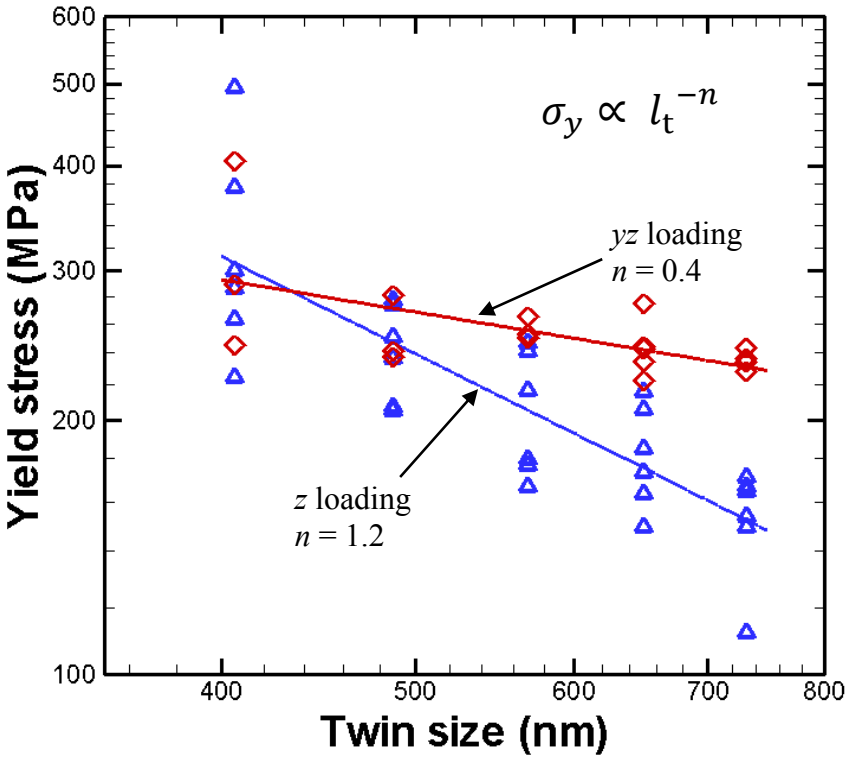

Figure 3. Variation of yield stress of twinned crystals with twin size (TB spacing).

CONCLUSIONS

A dislocation-$\{10\bar{1}2\}$ twin boundary interaction model that was introduced into discrete dislocation dynamics simulations was utilized to study the twin size effects in micro-twinned magnesium. Strong TB strengthening effect was captured, which was also observed to be orientation dependent. Basal slip orientation results in a strong twin size effect, while prismatic slip exhibits a weak effect.

ACKNOWLEDGMENTS

This research was sponsored by the Army Research Laboratory (#W911NF-12-2-0022). The views and conclusions contained in this document are those of the authors and should not be interpreted as representing the official policies, either expressed or implied, of ARL or U.S. Government. The U.S. Government is authorized to reproduce and distribute reprints for Government purposes notwithstanding any copyright notation herein. HF also gratefully acknowledges the financial support of Natural Science Foundation of China (11302140).

REFERENCES

1. J.W. Christian and S. Mahajan, *Prog. Mater. Sci.* **39**, 1 (1995).
2. L. Jiang, J.J. Jonas, A.A. Luo, A.K. Sachdev and S. Godet, *Mater. Sci. Eng. A* **445–446**, 302 (2007).

3. M. Knezevic, A. Levinson, R. Harris, R.K. Mishra, R.D. Doherty and S.R. Kalidindi, *Acta Mater.* **58**, 6230 (2010).
4. M.R. Barnett, Z. Keshavarz, A.G. Beer and D. Atwell, *Acta Mater.* **52**, 5093 (2004).
5. H. Fan, S. Aubry, A. Arsenlis and J.A. El-Awady, The role of twinning deformation on the hardening response of polycrystalline magnesium from discrete dislocation dynamics simulations (submitted).
6. E. Van der Giessen and A. Needleman, *Model. Simul. Mater. Sci. Eng.* **3**, 689 (1995).
7. H. Fan, Z. Li, M. Huang and X. Zhang, *Int. J. Solids. Struct.* **48**, 1754 (2011).
8. A. Arsenlis, W. Cai, M. Tang, M. Rhee, T. Oppelstrup, G. Hommes, T.G. Pierce and V.V. Bulatov, *Model. Simul. Mater. Sci. Eng.* **15**, 553 (2007).
9. L.P. Kubin, G. Canova, M. Condat, B. Devincre, V. Pontikis and Y. Brechet, *Solid State Phenom.* **23-24**, 455 (1992).
10. J.A. El-Awady, S. Bulent Biner and N.M. Ghoniem, *J. Mech. Phys. Solids* **56**, 2019 (2008).
11. H. Fan, Z. Li and M. Huang, *Scripta Mater.* **67**, 225 (2012).
12. C. Ouyang, Z. Li, M. Huang and H. Fan, *Int. J. Solids. Struct.* **47**, 3103 (2010).
13. Z. Li, C. Hou, M. Huang and C. Ouyang, *Comp. Mater. Sci.* **46**, 1124 (2009).
14. M. Huang, Z. Li and J. Tong, *Int. J. Plast.* **61**, 112 (2014).
15. H. Fan, Z. Li and M. Huang, *Scripta Mater.* **66**, 813 (2012).
16. C.C. Wu, P.W. Chung, S. Aubry, L.B. Munday and A. Arsenlis, *Acta Mater.* **61**, 3422 (2013).
17. G. Monnet, B. Devincre and L.P. Kubin, *Acta Mater.* **52,** 4317 (2004).
18. H. Fan, S. Aubry, A. Arsenlis and J.A. El-Awady, *Scripta Mater.* **97,** 25 (2015).
19. Z.H. Aitken, H. Fan, J.A. El-Awady and J.R. Greer, *J. Mech. Phys. Solids* **76**, 208 (2015).
20. L. Capolungo, I.J. Beyerlein and Z.Q. Wang, *Model. Simul. Mater. Sci. Eng.* **18**, 085002 (2010).
21. S. Olarnrithinun, S.S. Chakravarthy and W.A. Curtin, *J. Mech. Phys. Solids* **61**, 1391 (2013).
22. S. Groh, E.B. Marin, M.F. Horstemeyer and D.J. Bammann, *Model. Simul. Mater. Sci. Eng.* **17,** 075009 (2009).
23. Y. Tang and J.A. El-Awady, *Acta Mater.* **71**, 319 (2014).
24. S.R. Agnew and Ö. Duygulu, *Int. J. Plast.* **21**, 1161 (2005).
25. J. Zhang and S.P. Joshi, *J. Mech. Phys. Solids* **60**, 945 (2012).
26. Y. Tang and J.A. El-Awady, *Mater. Sci. Eng. A* **618**, 424 (2014).
27. H.-y. Song and Y.-l. Li, *Phys. Lett. A* **376**, 529 (2012).
28. J. Wang, I.J. Beyerlein and C.N. Tomé, *Int. J. Plast.* **56,** 156 (2014).
29. A. Serra and D.J. Bacon, *Phil. Mag. A* **73**, 333 (1996).
30. M. Yuasa, K. Masunaga, M. Mabuchi and Y. Chino, *Phil. Mag.* **94**, 285 (2013).
31. H. Fan, J.A. El-Awady and Q. Wang, *J. Nucl. Mater.* **458**, 176 (2015).
32. M.H. Yoo and C.-T. Wei, *Phil. Mag.* **14**, 573 (1966).
33. D.I. Tomsett and M. Bevis, *Phil. Mag.* **19**, 533 (1969).